crystals

MDPI

Article

A Study on the Mineralogy and Volatile Fraction of Scapolite from Mogok, Myanmar

Pengyu Yuan [1], Yi Zhao [2], Bo Xu [1,3,4,*] and Jiaqi Shen [1]

[1] School of Gemology, China University of Geosciences Beijing, 29 Xueyuan Road, Haidian District, Beijing 100083, China
[2] School of Earth Sciences and Resources, China University of Geosciences Beijing, 29 Xueyuan Road, Haidian District, Beijing 100083, China
[3] State Key Laboratory of Geological Processes and Mineral Resources, China University of Geosciences, Beijing 100083, China
[4] The Beijing SHRIMP Center, Chinese Academy of Geological Sciences, Beijing 100037, China
* Correspondence: bo.xu@cugb.edu.cn

Abstract: The Mogok metamorphic belt (MMB) of Myanmar is a famous geographical origin acknowledged by the whole world for its large mineral resources. In this study, basic gemological tests (density, UV fluorescence, refractive index, etc.), spectroscopic tests (infrared spectrum, Raman spectrum, and ultra-violet visible spectrum) and chemical composition analysis (electron microprobe and laser ablation inductively coupled plasma mass spectrometer) were carried out on scapolites from Myanmar. This paper explores the mineralogical characteristics of Burmese scapolites and provides additional information on its origin. Burmese scapolites are colorless and transparent with a yellow tone and belong to Cl-rich dipyre. The infrared spectra of the samples show the vibrations of Si-O and Al-O (400–1300 cm^{-1}), $(CO_3)^{2-}$ (1400–300 cm^{-1}), and OH (3048 cm^{-1} and 3568 cm^{-1}). The Raman spectra are mainly the vibrational spectra of Si (Al)-O-Si (Al) and the absorption peaks at 992 cm^{-1} and 1110 cm^{-1} caused by the vibrations of sulfate and carbonate ions, respectively. Black inclusions were found inside the scapolites, and the dark inclusions were identified as graphite by Raman spectroscopy. Moreover, the composition of the scapolite could be influenced by the $\alpha Cl^- / \alpha(CO_3)^{2-}$ of the fluid. The Cl activity degree could control the scapolite content as the ion exchange between scapolite and plagioclase was gradually balanced. The enrichment of rare earth elements and the apparent positive Eu anomaly indicate that Burmese scapolites have a high degree of light and heavy rare earth element differentiation and an oxidizing environment of mineralization.

Keywords: scapolite; Myanmar; Raman spectroscopy; inclusions; LA-ICP-MS; volatile fraction

Citation: Yuan, P.; Zhao, Y.; Xu, B.; Shen, J. A Study on the Mineralogy and Volatile Fraction of Scapolite from Mogok, Myanmar. *Crystals* **2022**, *12*, 1779. https://doi.org/10.3390/cryst12121779

Academic Editor: Elena Sturm

Received: 26 October 2022
Accepted: 18 November 2022
Published: 7 December 2022

1. Introduction

Scapolite has been considered to be a common mineral for a long time. It was not until 1913 that gem-quality scapolites were first discovered in Burma. Gem-quality scapolites of various colors were continuously reported and came into public view [1]. Gem-quality scapolites usually have good clarity, remarkable size, and a wide variety of colors, including colorless, yellow, orange, pink, blue, purple, yellow–green, and pink–purple. Despite the hardness of scapolite being relatively low (Mohs hardness is 5–6), it is very attractive as a collection. The most significant sources of gem-quality scapolites are Afghanistan (Badakhshan), China (Xinjiang-Uygur Autonomous Region), Brazil, Sri Lanka, Pakistan, Myanmar (Mogok), and Mozambique [1].

The scapolite group of minerals includes widely distributed aluminosilicate rock-forming minerals, which are extensively reported in nature. The chemical molecular general formula of scapolite is $M_4T_{12}O_{24}A$, and the main components are M = Na and Ca, T = Si and Al, and A = Cl, CO_3^{2-}, and SO_4^{2-}. The composition of scapolite is generally considered to be a solid solution composed of four end members: a sodium chloride

end member, marialite ($Na_4Al_3Si_9O_{24}Cl$); two calcium carbonate end members, meionite ($Ca_4Al_6Si_6O_{24}CO_3$) and mizzonite ($NaCa_3Al_5Si_7O_{24}CO_3$); and a calcium sulfate end member, sulphate meionite ($Ca_4Al_6Si_6O_{24}SO_4$) [2,3]. Pure marialite has a high stabilization temperature (the formation temperature is more than 700 °C), which cannot be found in nature. All natural Na-rich scapolites contain Me components, which are formed under relatively low temperature and pressure conditions, with temperatures mostly less than 700 °C and pressures mostly 5–8 kbar [4]. In regional metamorphic rocks, they are often regarded as one of the minerals in the mineral phase assemblage of the metamorphic peak, and they are sometimes treated as metasomatic minerals [3]. Unlike other chlorine-containing minerals (such as hornblende, mica, and apatite), scapolite is virtually without OH. Thus, it can be used as a tracer for the contents of Cl and CO_2 in fluids but is not related to f_{H2O} [2]. The scapolite is chemically stable due to its ability to combine with volatiles (Cl, CO_2, and SO_3). It is a crucial mineral to solve problems related to volatile components of underlying crustal processes, even in high temperature and pressure conditions of granite facies. The relative prevalence and abundance of scapolite in metamorphic rocks and hydrothermal altered igneous rocks indicate that this mineral has an extensive and stable distribution [5].

In this paper, we studied the scapolite from Myanmar (Mogok). Since the report of Burmese scapolite in 1913, there is still a shortage of spectroscopic studies related to Burmese scapolite. Furthermore, there is no well-established gemological system, and there is a lack of information on the origin of Mogok scapolite. Therefore, the basic gemology, spectroscopy, and major and trace elements of the Mogok scapolite were analyzed in this study. The gemological characteristics, spectral characteristics, and coloring causes of Burmese scapolite were clarified through this research, and the mineral types of inclusions were determined. The volatile fractions in the scapolite were also investigated to explore the compositional characteristics of scapolite.

2. Geological Setting

High-grade granite and overlying diorite marble constitute the major part of the Mogok metamorphic belt (MMB) in Myanmar. The metamorphic belt extends southward from the eastern Himalayas, passing though the eastern Kachin State and Mogok region and extending to Mandalay (Figure 1) [6]. The geology setting of Mogok is very complex, mainly composed of high-grade metamorphic schist and gneiss; granite intrusions, including gem-bearing pegmatite; ultramafic rocks containing olivine; and metamorphic marble containing ruby and spinel [7,8].

Gneiss is the main rock unit in Mogok, which is composed of various types of metamorphic rocks, including scapolite-bearing and garnet-bearing biotite gneiss, calcareous gneiss, hornblende schist, and schist. Marble is the main host rock of ruby and spinel, closely interbedded with Mogok gneiss. The scapolite forms mainly in the metamorphic marble region (in the form of scapolite or pyrite–scapolite–diopside marble). Granite intrusions occupy one third of the rock belt in western Mogok, which consists of Kabaing granite, augite and hornblende granite, and syenite and tourmaline granite. Pegmatites with tourmaline, topaz, and aquamarine are also included in this zone. In Mogok, basic intrusions are rare, limited to gabbros and hornblende-pyroxenites, as well as peridotites found in Bernardmyo, 10 km north of Mogok, as secondary intrusive dikes and beds. In the olivine deposits, the rocks usually form a series of loose weathered deposits with serpentinization on the surfaces. The marble usually crystallizes very coarsely with pure white in color, and some may be locally tinged with yellow or pink. In addition to ruby and spinel, marble also contains diopside, phlogopite, olivine, scapolite, titanite, garnet, and graphite. Granite intrudes into marble, and the influence of contact metamorphism is manifested in the presence of feldspar and diopside in the coarse-grained portion contacting the granites [7–11].

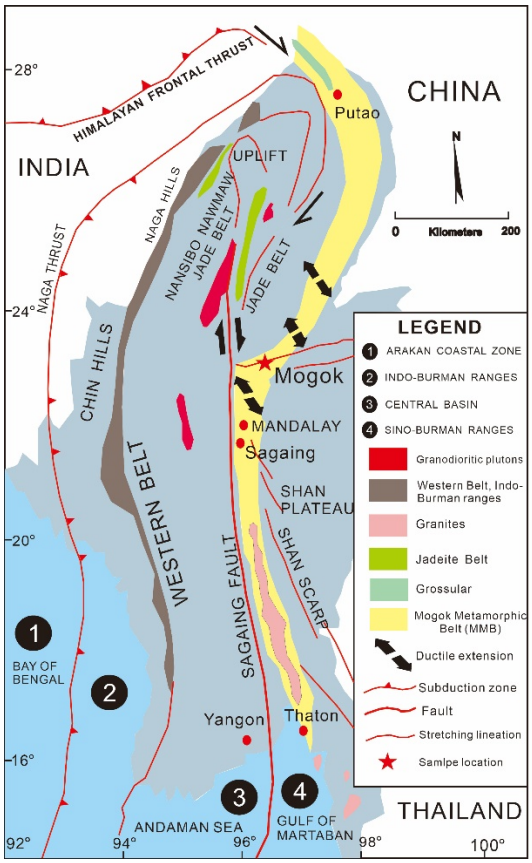

Figure 1. Geological Map of Mogok area (Principle geological features of Myanmar and Mogok). Modified from [9] and the references from it. (Scapolites sampling site was marked on the figure).

3. Materials and Methods

Gemological tests, spectroscopic tests, and chemical composition tests were conducted on scapolite U-1 and U-2 from Myanmar.

The samples were photographed, micro-graphed, and routinely gemological tested at the Gem Identification Laboratory of China University of Geosciences (Beijing). The scapolite U-1 and U-2 were selected for refractive index and birefringence measurements on polished and flat faces, and the refractive oil was diiodomethane. The fluorescence was observed by ultraviolet fluorescent lamps with a long wavelength of 365 nm and a short wavelength of 254 nm. The hydrostatic method was used to measure the relative density of the samples.

Infrared spectra, Raman spectra, and UV–visible spectra were tested at the Gemological Experimental Center of China University of Geosciences (Beijing). A flat surface was selected to polish, and two points from the center and edge of the sample were chosen for spectroscopic testing. A German BRUKER TENSOR27 Fourier transform infrared (FTIR) spectrometer was used to measure the infrared spectrum of the samples. The reflection method was adopted for the test as following: the test range was from 400 cm^{-1} to 2000 cm^{-1}, the scanning signals of the sample and the background were accumulated 32 times, the resolution was 4 cm^{-1}, the scanning voltage was 85–265 V, the temperature had a range of 18–25 °C, and the humidity was <70%. In addition, the infrared spectra of the samples after 2000 cm^{-1} were tested by a German BRUKER LUMOS micro-infrared spectrometer (Micro-FTIR). Since the samples were relatively transparent and of moderate thickness, they could be tested directly by micro-FTIR. The transmission method was used: the resolution was 8 cm^{-1}, the scanning time of the sample and background was 12 times, and the testing range was 2000–4000 cm^{-1}.

The Raman spectra were tested by HORIBA HR-Evolution microscopic Raman spectrometer from Japan. The test wavelength: 532 nm, the scanning range: 400–4000 cm^{-1}, the resolution: 4 cm^{-1}, and the laser power: 50 mW. UV–visible spectrophotometer (UV–VIS) UV-3600 from Kyoto Shimadzu Corporation, Japan, was used for UV-VIS. The wavelength range is 300–900 nm, with high-speed scanning, sampling interval 1 s, slit width 20 nm, and single scanning mode. The use of these tests can better clarify the spectroscopic characteristics of Burmese scapolites.

The major element compositions of Myanmar scapolite U-1 and U-2 were determined by an electron microprobe analysis (EMPA) instrument of type JXA-8230 in the Electronic Probe Laboratory of China University of Geosciences (Beijing, China). The samples were mechanically crushed. The part of the samples with no inclusions inside was selected under the binoculars, after which they were placed in epoxy resin blocks and polished. The polished samples were surface carbon blasted before testing. The test conditions were: electron beam current 2×10^{-8} A, beam spot 5 μm, acceleration voltage 15 kV, elemental test accuracy >0.001%.

A laser ablation inductively coupled plasma mass spectrometer (LA-ICP-MS) at the Institute of Geomechanics, Chinese Academy of Geological Sciences was applied to measure the trace elemental composition of the samples. A 193 nm excimer laser exfoliation system (GeoLas HD, Coherent, Saxonburg, PA, USA) and a four-stage rod mass spectrometer (Agilent 7900) form the main part of the LA-ICP-MS. Ablation is carried out in helium atmosphere. ICP-MS is adjusted to ensure stable plasma conditions and low oxide generation level. LA-ICP-MS is able to measure the trace element content of samples more accurately and in a shorter time. Clean the target previously used for EMPA measurement to avoid the influence of residual carbon on the results. A repetition frequency of 5 Hz at an energy of 90 mJ was used for scapolites. NIST 612 and NIST 610 glasses were utilized to standardize all elements analyzed.

4. Results

4.1. Visual Appearance and Gemological Properties

The Burmese scapolites U-1 and U-2 were nearly colorless with a yellow tint. They exhibited a medium glassy luster and transparency. The samples were columnar in overall shape. The crystals were large (the length of U-1 was 3.4 cm, and the thickness was 1.1 cm; the length of U-2 was 3.6 cm, and the thickness was 0.8 cm), well crystallized (Figure 2a, b), with uneven longitudinal lines on the surface and shell-like fractures in the cross section (Figure 2c). Under the gem microscope, there were dark granular inclusions and dark short columnar solid inclusions in U-1, and gas–liquid inclusions in U-2 (Figure 2d–f). In addition, many cracks occurred in the samples, in which color film interference could be seen.

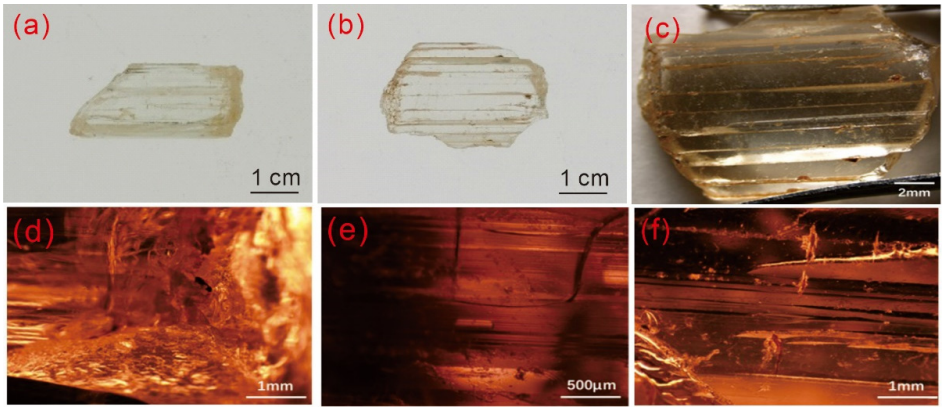

Figure 2. (**a**,**b**) Scapolite crystals ((**a**) is U-1; (**b**) is U-2). (**c**) Crystalline longitudinal pattern of scapolite. (**d**,**e**) Black solid inclusions and short columnar inclusions in U-1. (**f**) Gas–liquid two-phase inclusions in U-2.

The refractive index of scapolite was measured by a gem refractometer. The average refractive index of U-1 was 1.556, and the average birefringence was 0.015–0.020. The average refractive index of U-2 was 1.560, and the average birefringence was 0.010–0.020. The polychromatic property of U-1 was not obvious, while that of U-2 was colorless–light yellow. U-1 and U-2 showed strong pink–purple fluorescence under the long wavelength of the ultraviolet fluorescence instrument, while they showed strong pink fluorescence under the short wavelength (Figure 3). The relative densities of U-1 and U-2 were 2.657 and 2.645, respectively.

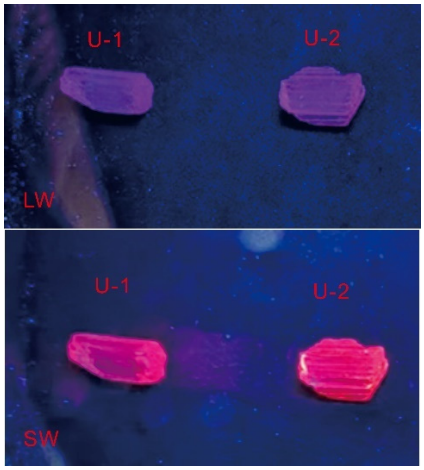

Figure 3. UV fluorescence characteristics of U-1 and U-2 with different colors in long and short wavelengths UV lamp.

4.2. Spectral Characteristics

4.2.1. Infrared Spectrum

The structure of silicate minerals is formed by the polymerization of Si-O tetrahedral corner-sharing vertices, and Al often replaces Si in Si-O tetrahedra. Therefore, in the infrared spectrum of silicates, Si-O and Al-O vibrations are predominant. The scapolite group minerals belong to a fully homogeneous series with substitution between Na^+ and Ca^{2+}, in addition to the frequent substitution of Si in the structure by Al. Because the radius, charge, and chemical bond strength of the ions before and after substitution are different, the size and symmetry of the coordination tetrahedra change, which may cause lattice distortion, splitting, and shifting of the spectral bands [12]. Scapolite is a kind of feldspathoids mineral, which has a high similarity with feldspar. There has been little study on the attribution of scapolite peak position. Therefore, the position determination in this paper was carried out in combination with the infrared spectra of feldspar and meionite.

In the range of 400–1300 cm^{-1}, four groups of data for Myanmar scapolite U-1 and U-2 all showed nine groups of infrared spectrum peaks (Figure 4a): 415, 455, 550, 621, 752, 1035, 1109, and 1209 cm^{-1}. The absorption band of 415 cm^{-1} was attributed to the bending vibration of Si-O-Si. The strong bands around 455 cm^{-1} and 550 cm^{-1} were related to the coupling of the Si-O-Si bending vibration and the Na (7yCa)-O stretching vibration. The sharp band near 621 cm^{-1} was due to the O-Si-O bending vibration. The weak absorption bands near 688 cm^{-1} and 752 cm^{-1} were generated by the Si-Al (Si) stretching vibrations. The strong band of 1035 cm^{-1} was correlated with the stretching of Si (Al)-O vibrations. The wide bands around 1109 cm^{-1} and 1209 cm^{-1} were associated with the stretching vibration of Si-O. Magnifying the wavenumber in the range of 1400–1600 cm^{-1} showed that the samples had a weak absorption band near 1528 cm^{-1}, which was caused by the stretching vibration of CO_3^{2-} (Figure 4b). The infrared spectrum of scapolites in the range of 2400–3700 cm^{-1} is shown in Figure 4c. The absorption bands at 2502 cm^{-1}, 2540 cm^{-1}, and 2628 cm^{-1} were caused by the symmetric and antisymmetric stretching and combining frequency vibration of CO_3^{2-}. The first-order frequency doubling peak of

CO_3^{2-} in antisymmetric stretching vibration occurred near 2963 cm^{-1}. In particular, the absorption peak at 3048 cm^{-1} was caused by the M-OH stretching vibration; 3586 cm^{-1} was due to the O-H symmetric stretching vibration [12].

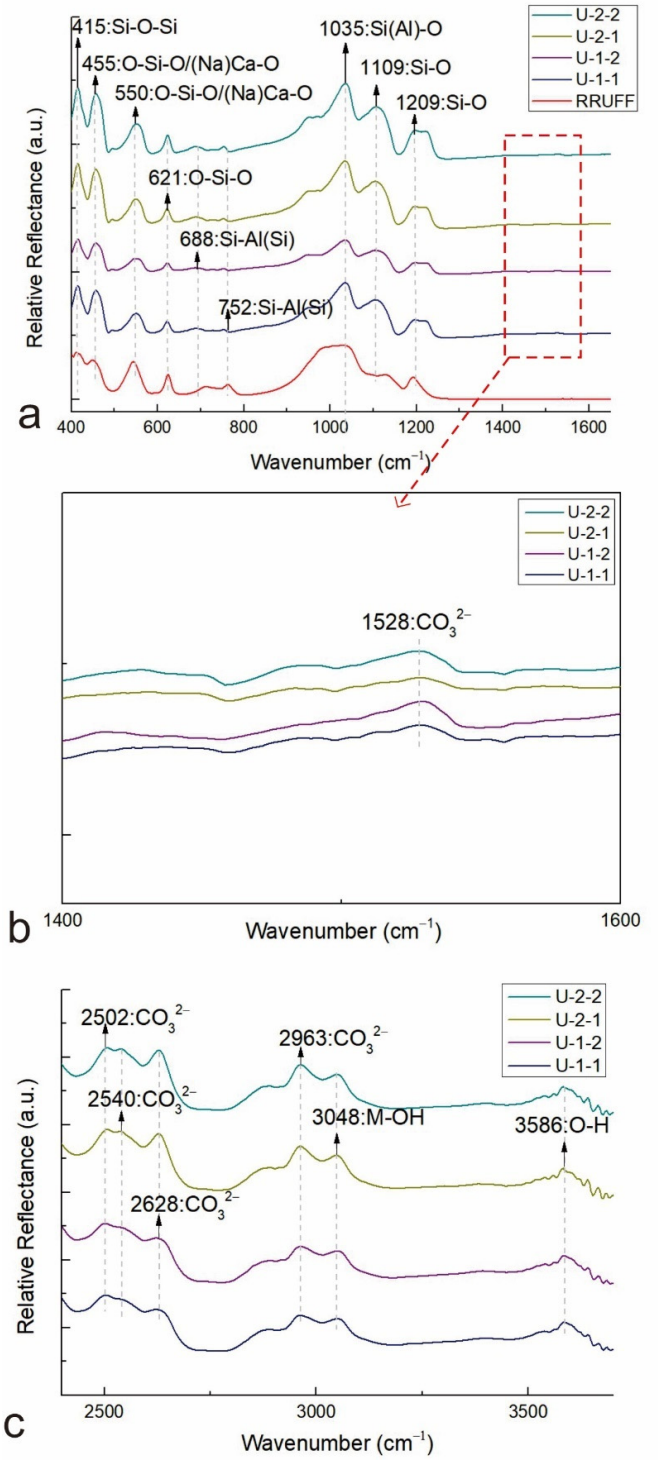

Figure 4. (**a**) Infrared spectra of scapolite from Mogok measured by FTIR. (**b**) Infrared spectra of samples in the range of 1400–1600 cm^{-1} measured by FTIR. (**c**) The infrared spectrum of samples in the range of 2400–3700 cm^{-1} was measured by micro-FTIR. (From RRUFF database: R050123 from Pakistan; U-1-1 is the center test point of the sample, U-1-2 is the edge test point of the sample; U-2-1 and U-2-2 are the same).

Comparison with the scapolite of R050123 (from Pakistan) in the RRUFF database showed that the spectral peaks of samples were basically consistent with it. Burmese scapolite U shifted to the left near 1109 cm^{-1}, and the absorption band of the sample near 1209 cm^{-1} was wider than R050123. The testing range of infrared reflectance spectra was 400–2000 cm^{-1}. The region reflecting the vibration information of the mineral framework and the whole vibrational band could determine the species of the gemstone. The samples studied in this paper were scapolite from the same origin, so the reflection spectra were consistent.

4.2.2. Raman Spectrum

The four groups of Raman spectra of scapolite U-1 and U-2 were basically the same, with sharp peaks, indicating the high degree of crystallization of the samples. The Raman spectrum of scapolite U was mainly concentrated in the range of 200–1200 cm^{-1}. Thirteen groups of Raman activity peaks (v_1–v_{13}) were collected from the test (Figure 5). The peaks less than 400 cm^{-1} were due to the vibration between cations and O and the lattice vibration between mineral lattice frameworks. The Raman shifts of the samples in the low frequency range were mainly 107–128 cm^{-1} (v_1), 162 cm^{-1} (v_2), 189 cm^{-1} (v_3), 223 cm^{-1} (v_4), 262 cm^{-1} (v_5), 286 cm^{-1} (v_6), 335 cm^{-1} (v_7), and 358 cm^{-1} (v_8). Due to the influence of Al^{VI}, the Raman spectrum of the low frequency peaks was split, and v_4 was generated by the splitting of v_3 and v_5, and v_6, v_7, and v_8 were generated by the splitting. The strongest peak at 458 cm^{-1} (v_9) was associated with the Si-O-Si bridging oxygen bending vibration. The mid-strong Raman peak near 536 cm^{-1} (v_{10}) was caused by the bending vibration of bridging oxygen in Al-O-Si. The band at 773 cm^{-1} (v_{11}) was generated by the antisymmetric stretching vibration between Al-O_{br}-Al, which was due to the fourth coordination of Al. The adsorption peak near 992 cm^{-1} (v_{12}) was caused by the symmetric stretching vibration of the sulfate ion. Furthermore, the weak spectral peak at 1110 cm^{-1} (v_{13}) was owing to the v_1 symmetric stretching vibration of the carbonate ion [13,14].

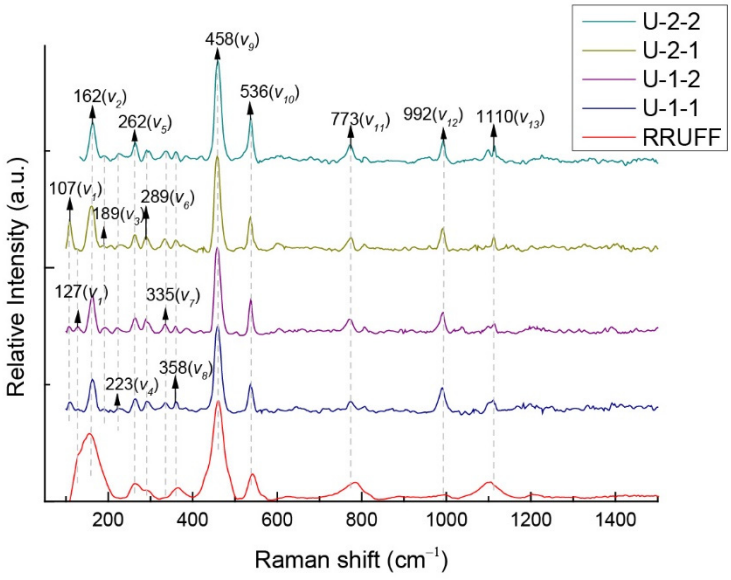

Figure 5. Raman spectrum of scapolite from Mogok. (From RRUFF database: R050123 from Pakistan; U-1-1 is the center test point of the sample, U-1-2 is the edge test point of the sample; U-2-1 and U-2-2 are the same. There are 13 groups of Raman spectral peaks in the samples and they are consistent with R050123).

Comparing the samples with R050123, it was found that the Raman spectral peaks were basically coincident, and the intensity of the peaks was slightly different. The splitting of the samples was more obvious in the low frequency region below 400 cm^{-1}, presumably

due to the higher order of Burmese scapolites Al. The highest diffraction peaks could be seen around 458 cm^{-1}, and the intensities were quite close to each other. R050123 is a marialite from Pakistan, which indicates that the Raman spectra of Burmese scapolites are similar to marialite.

4.2.3. UV–Vis Spectrum

Burmese scapolite U appeared to be colorless (with a yellowish hue). The samples had absorption peaks at 380 nm, 418 nm, 446 nm, and 472 nm (Figure 6). The absorption peaks below 400 nm were not within the visible range and had no influence on the color of the samples observed by the naked eye. The 418 nm absorption peak could absorb violet light and allows yellow–green light to pass through, thus making the sample appear green and yellow. The absorption peak at 446 nm could absorb blue light, make yellow light pass through, and then make the sample appear yellow. Thus, the Burmese scapolites have a yellow hue due to absorption near 418 nm and 446 nm.

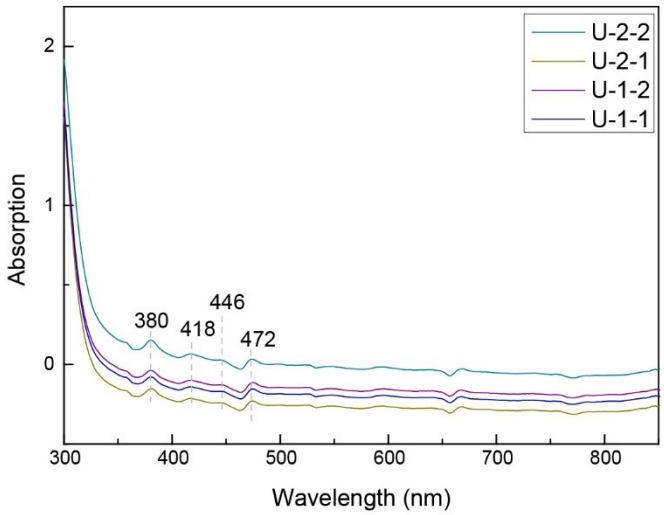

Figure 6. UV–visible spectrum of scapolite from Mogok. (Both scapolite samples had absorption peaks at 380 nm, 418 nm, 446 nm and 472 nm).

There are two main reasons for the color of scapolite: color-centered coloration, and coloration by electron leap of transition metal ions. The yellow color of scapolite is due to the small radius of Fe^{3+}, which can replace Al and Si in the crystal lattice, resulting in absorption peaks around 377 nm, 417 nm, 442 nm, and 483 nm [15–18]. Scapolite is a kind of feldspathoids mineral, and its silicon–oxygen tetrahedron framework is connected in a similar way to that of feldspar. The positions of Al and Si can be replaced by Fe^{3+}, which has an electronic grouping of $3d^5$ and only one six-fold simplification of the ground state energy level $^6A_1$. Burmese scapolites U-1 and U-2 exhibit are colorless as a whole but have a light yellow hue, so their yellow hue may be attributed to the electronic transition between Fe^{3+}. The peak around 380 nm is due to the $^6A_1$–^4E (^4D) transition of Fe^{3+}. The wide FWHM of the peak at 418 nm is due to the $^6A_1$–$^4T_2$ (^4D) transition. The absorption at 446 nm is caused by the $^6A_1$–$^4A_1{}^4E$ (^4G) transition. The 472 nm absorption is caused by the $^6A_1$–$^4T_2$ (^4G) transition [15,18,19]. In addition, Burmese scapolites may form mineral assemblages with other minerals (pyrite and diopside), so the yellow hue of the samples may also be contaminated by Fe-containing substances.

4.3. Inclusions

Dark solid inclusions appeared in Burmese scapolite U-1 and U-2 studied in this paper. The inclusions were tested using laser Raman spectroscopy, and the spectral results are shown in Figure 7. Compared with the standard spectra in the laser Raman database, the solid inclusions in U-1 and U-2 could be identified as graphite. For crystalline graphite,

the Raman spectrum was dominated by a strong scattering ("O" peak) at 1582 cm^{-1}, two stronger peaks at near 2735 and 2695 cm^{-1}, and two weak peaks at near 2440 and 3250 cm^{-1}. Disordered carbon also had three peaks around 1360 cm^{-1} (D), 1620 cm^{-1} (D'), and 2960 cm^{-1} (D") [20].

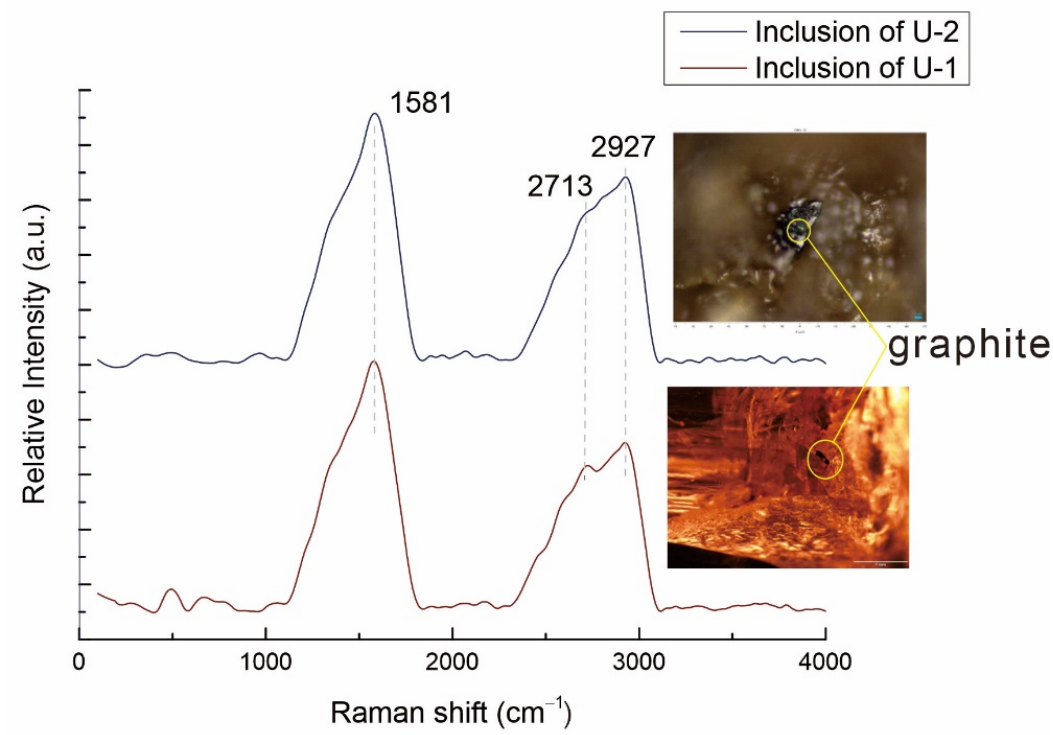

Figure 7. Black inclusions in U-1 and U-2 and their Raman spectra. (The upper Raman spectrum shows the black inclusion in U-1, and the lower one shows the inclusion in U-2).

As seen from the spectra, the main Raman shifts of the dark inclusions appeared near 1581 cm^{-1}, 2713 cm^{-1}, and 2927 cm^{-1}, which matched the Raman spectral peaks of graphite. According to its characteristics, it could be determined that the inclusions in scapolite are graphite.

4.4. Major and Trace Element Compositions

The results of the electron probe test showed (Table 1) that Burmese scapolite U-1 contained 51.76 wt% SiO_2, 8.42 wt% Na_2O, and 22.79 wt% Al_2O_3; U-2 contained 51.59 wt% SiO_2, 8.51 wt% Na_2O, and 23.06 wt% Al_2O_3. In addition, the Cl content of U-1 was 2.64 wt% (0.68 apfu), and the SO_3 concentration was 1.02 wt% (0.12 apfu). The Cl content of U-2 was 2.64 wt% (0.68 apfu), and the SO_3 concentration was 1.09 wt% (0.13 apfu). Meionite content could also be used to define the series of scapolite. The formula Me% = 100 × Ca/(Na + Ca) [20] was used for calculation, and the results are shown in Table 1. The scapolite U had a Me% range of 34.95 to 36.36%, and a Ma% range of 63.64 to 65.05%. Therefore, it could be judged that Myanmar scapolite is dipyre. The chemical general formula of the scapolite group minerals is $X_4[Y_{12}O_{24}]Z$; X = Na^+, K^+, and Ca^{2+}; Y = Si^{4+} and Al^{3+}; Z = Cl^-, F^-, OH^-, CO_3^{2-}, and SO_4^{2-}. Sulfur in scapolite can be present either as SO_3^{2-} and SO_4^{2-} substituted for CO_3^{2-} or as S^{2-} because its ionic radius is similar to that of Cl [21,22]. The crystal chemical formula of Burmese scapolites could be obtained by calculating the average value of sample points based on Si + Al = 12 (Table 1). U-1 is $(Na_{2.49}\ Ca_{1.40}\ K_{0.28})\ (Al_{4.10}\ Si_{7.90})\ O_{24}\ (Cl_{0.68}\ (CO_3)_{0.20}\ (SO_4)_{0.12})$; U-2 is $(Na_{2.51}\ Ca_{1.41}\ K_{0.31})\ (Al_{4.14}\ Si_{7.86})\ O_{24}\ (Cl_{0.68}\ (CO_3)_{0.19}\ (SO_4)_{0.13})$.

Table 1. Electron microprobe analysis of scapolite from Myanmar (Mogok) and cations calculated on the basis of Si + Al = 12.

	U-1-1	U-1-2	U-1-3	U-1-4	U-1-5	U-2-1	U-2-2	U-2-3	U-2-4	U-2-5
SiO_2	51.67	51.76	52.08	51.89	51.39	50.97	51.98	51.64	51.64	51.73
Al_2O_3	22.79	22.70	22.70	22.60	23.17	22.73	23.23	23.09	23.22	23.03
CaO	8.74	8.46	8.39	8.33	8.68	8.58	8.63	8.67	8.63	8.45
Na_2O	8.69	8.26	8.31	8.32	8.54	8.40	8.37	8.53	8.55	8.71
K_2O	1.33	1.50	1.54	1.52	1.41	1.58	1.49	1.53	1.71	1.54
Cr_2O_3	0.01	bdl	bdl	bdl	0.03	bdl	bdl	bdl	bdl	0.01
TiO_2	0.01	0.02	0.01	0.03	bdl	0.07	bdl	bdl	bdl	0.02
MgO	0.03	0.02	0.01	0.02	bdl	0.04	0.02	0.02	0.03	0.03
FeO	0.10	0.20	0.16	0.06	0.21	0.09	0.16	0.12	0.09	0.13
MnO	bdl	bdl	0.02	bdl	0.02	bdl	0.04	0.07	0.07	bdl
NiO	bdl	bdl	0.02	0.04	0.02	bdl	bdl	0.05	0.03	0.11
K_2O	1.33	1.50	1.54	1.52	1.41	1.58	1.49	1.53	1.71	1.54
ZnO	0.06	0.11	0.04	0.02	bdl	bdl	bdl	bdl	0.11	bdl
Cl	2.57	2.66	2.63	2.69	2.64	2.73	2.55	2.69	2.62	2.61
F	bdl	bdl	bdl	bdl	bdl	bdl	0.07	0.01	bdl	0.12
SO_3	1.26	0.92	0.96	0.95	1.03	1.26	1.14	1.01	1.08	0.97
Total	97.26	96.61	96.88	96.44	97.13	96.46	97.68	97.42	97.78	97.45
Cations calculated on the Basis of Si + Al = 12 (apfu)										
Si^{4+}	7.90	7.91	7.93	7.93	7.84	7.86	7.86	7.86	7.84	7.87
Al^{3+}	4.10	4.09	4.07	4.07	4.16	4.14	4.14	4.14	4.16	4.13
Ca^{2+}	1.43	1.39	1.37	1.37	1.42	1.42	1.40	1.42	1.41	1.38
Na^{+}	2.57	2.45	2.45	2.46	2.53	2.51	2.45	2.52	2.52	2.57
K^{+}	0.26	0.29	0.30	0.30	0.27	0.31	0.29	0.30	0.33	0.30
Cl^{-}	0.67	0.69	0.68	0.70	0.68	0.71	0.65	0.69	0.67	0.67
SO_3	0.14	0.11	0.11	0.11	0.12	0.15	0.13	0.12	0.12	0.11
CO_2	0.19	0.21	0.21	0.20	0.20	0.14	0.22	0.19	0.20	0.22
Me	35.78	36.19	35.87	35.67	36.00	36.13	36.36	35.99	35.86	34.95
Ma	64.22	63.81	64.13	64.33	64.00	63.87	63.64	64.01	64.14	65.05
EqAn	36.82	36.33	35.77	35.70	38.81	37.84	38.01	38.08	38.58	37.66
XCl	66.62	68.83	67.93	69.63	68.15	71.40	65.41	69.31	67.48	67.39

bdl = below detection limit.

The test results of trace elements of Burmese scapolite are shown in Table 2. The Burmese scapolites had high contents of Na, Al, and Ca, while the Mg content ranged from 55.34 ppm to 69.17 ppm, the Fe content ranged from 453.06 ppm to 620.47 ppm, and the Mn content ranged from 125.90 ppm to 140.90 ppm. Normalized for the upper continental crust (UCC) for rare earth elements (REEs) (Figure 8a), the samples exhibited an overall right-sloping distribution with obvious positive Eu anomalies, and the range of δEu was 2.11–3.42. There was no significant Ce anomaly, and the δCe value of the samples was about 1. Moreover, ΣREE of the samples was 38.37–45.51 ppm, the range of ΣLREE was 36.80–43.58 ppm, and the range of ΣHREE was 1.43–1.93 ppm. Figure 8b demonstrates the normalized illustration of the upper continental crust of the scapolites, and it was shown that Burmese scapolites were enriched in large ion lithophile elements (Rb, Sr, and K) and

depleted in high field-strength elements (Th and Ta). Additionally, most trace elements were normalized to values below 1, suggesting that many of the trace elements in the scapolites were lower in content than in the UCC.

Table 2. Chemical compositions of scapolite from Myanmar (Mogok) analyzed by LA-ICP-MS.

		U-1-1	**U-1-2**	**U-1-3**	**U-1-4**	**U-1-5**	**U-1-6**	**U-1-7**	**U-2-1**	**U-2-2**	**U-2-3**	**U-2-4**	**U-2-5**	**U-2-6**	**U-2-7**
Na	ppm	34,356.71	34,089.81	31,799.44	33,679.55	31,318.06	34,242.48	34,526.41	35,338.46	34,938.31	34,952.24	34,042.80	34,818.52	34,723.40	35,307.30
Mg	ppm	66.43	63.94	55.34	67.46	61.55	69.17	69.09	67.17	66.16	64.04	61.76	65.38	64.38	63.92
Al	ppm	74,588.00	73,469.03	70,161.98	74,858.76	71,187.64	76,915.30	76,601.09	77,689.37	76,902.61	75,779.13	72,552.90	76,367.61	76,478.47	74,636.92
SiO_2	wt%	29.09	29.62	26.31	28.49	27.18	29.16	29.88	30.33	30.58	29.96	29.51	29.96	30.20	30.69
K	ppm	6723.65	6397.20	5511.72	6454.82	5803.90	7872.44	8046.27	8186.85	8199.78	8033.47	7834.38	7887.11	7782.00	8126.78
Ca	ppm	36,157.23	35,650.46	34,032.92	35,853.02	34,276.60	35,714.60	35,707.90	36,344.73	35,683.09	35,252.81	33,559.24	35,470.80	35,868.06	34,892.29
Mn	ppm	133.42	131.14	123.63	133.50	125.90	138.69	139.57	140.90	140.82	134.57	127.40	132.87	131.14	131.20
Fe	ppm	540.38	525.72	453.06	542.75	508.46	598.83	605.47	620.85	603.53	594.00	584.67	592.71	583.33	591.21
Zn	ppm	14.77	11.02	11.40	12.82	9.38	8.54	7.11	9.21	7.20	10.44	9.86	8.17	7.84	8.92
Ga	ppm	11.05	11.25	10.32	10.50	9.90	10.61	11.03	10.59	11.38	10.20	10.50	9.96	11.53	10.92
Rb	ppm	7.84	7.23	5.99	7.41	6.79	7.63	6.73	7.51	6.72	6.84	6.25	6.52	6.17	6.69
Sr	ppm	224.71	229.72	218.32	218.41	218.23	295.07	292.89	295.86	292.24	352.70	330.74	348.30	354.58	342.84
Y	ppm	2.57	2.47	2.11	2.65	2.29	2.33	2.25	2.24	2.13	2.22	2.21	2.40	2.41	2.30
Ba	ppm	28.23	26.75	26.97	28.02	26.46	36.36	37.45	35.99	36.33	44.40	43.10	41.87	47.15	43.04
La	ppm	11.93	11.91	10.64	11.23	11.47	11.37	11.01	11.81	11.04	12.07	11.59	12.30	12.41	12.49
Ce	ppm	19.85	19.31	17.66	19.59	18.91	19.20	18.79	19.28	19.08	19.60	19.09	20.00	20.49	19.52
Pr	ppm	1.81	1.90	1.63	2.02	1.71	1.90	1.98	1.98	1.80	1.95	1.85	2.14	1.99	1.85
Nd	ppm	6.43	6.32	5.59	6.21	6.52	6.37	6.56	6.09	6.68	7.35	6.36	7.06	7.12	6.48
Sm	ppm	0.81	0.77	0.82	0.95	1.27	1.27	0.95	0.75	0.88	1.02	1.07	0.90	1.09	1.00
Eu	ppm	0.42	0.43	0.47	0.46	0.43	0.65	0.53	0.48	0.53	0.52	0.56	0.59	0.48	0.60
Gd	ppm	0.80	0.61	0.73	0.65	0.64	0.53	0.76	0.65	0.73	0.91	0.53	0.65	0.90	0.79
Tb	ppm	0.12	0.10	0.08	0.10	0.07	0.09	0.10	0.09	0.06	0.08	0.07	0.09	0.09	0.09
Dy	ppm	0.48	0.30	0.37	0.40	0.28	0.56	0.46	0.38	0.43	0.44	0.43	0.32	0.52	0.50
Ho	ppm	0.09	0.09	0.07	0.09	0.06	0.06	0.07	0.04	0.06	0.08	0.07	0.10	0.07	0.07
Er	ppm	0.22	0.19	0.20	0.21	0.16	0.21	0.17	0.28	0.21	0.13	0.17	0.23	0.15	0.19
Tm	ppm	0.04	0.02	0.01	0.01	0.02	0.02	0.01	0.02	0.02	0.01	0.04	0.02	0.03	0.01
Yb	ppm	0.15	0.17	0.10	0.26	0.19	0.26	0.06	0.11	0.18	0.12	0.11	0.18	0.15	0.23
Lu	ppm	0.00	0.02	0.01	0.02	0.02	0.01	0.01	0.04	0.01	0.03	0.03	0.06	0.01	0.05
Hf	ppm	0.00	0.00	0.01	0.00	0.00	0.00	0.00	0.01	0.00	0.00	0.00	0.00	0.00	0.00
Ta	ppm	0.00	0.00	0.01	0.00	0.00	0.00	0.00	0.00	0.01	0.00	0.01	0.01	0.00	0.00
Pb	ppm	12.14	14.72	14.64	11.47	13.12	13.49	13.55	14.23	13.87	17.80	17.65	17.89	17.97	17.99
Th	ppm	0.00	0.00	0.01	0.01	0.01	0.00	0.01	0.00	0.00	0.00	0.01	0.01	0.01	0.00
U	ppm	0.00	0.00	0.00	0.00	0.00	0.00	0.01	0.00	0.00	0.00	0.01	0.01	0.00	0.01
δEu		2.23	2.73	2.62	2.53	2.05	3.42	2.73	2.96	2.88	2.34	3.23	3.35	2.11	2.91
δCe		1.01	0.96	1.00	0.97	1.00	0.97	0.95	0.94	1.00	0.95	0.97	0.92	0.97	0.96
ΣREE	ppm	43.15	42.13	38.37	42.18	41.76	42.50	41.45	41.99	41.73	44.31	41.94	44.64	45.51	43.88
ΣLREE	ppm	41.24	40.64	36.80	40.46	40.32	40.76	39.83	40.39	40.02	42.51	40.51	43.00	43.58	41.95
ΣHREE	ppm	1.91	1.49	1.57	1.73	1.44	1.74	1.63	1.60	1.72	1.80	1.43	1.64	1.93	1.92

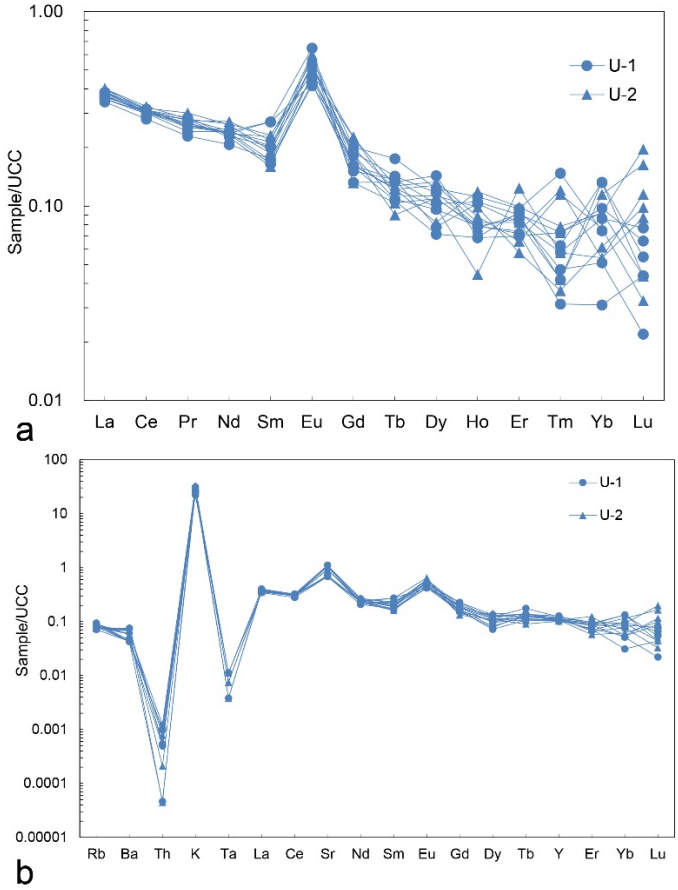

Figure 8. (**a**) Average upper continental crust (UCC)-normalized REE distribution patterns of scapolite (Mogok). The normalization values for upper crust from Rudnickand and Gao (2003) [23]. (**b**) Average upper continental crust (UCC) normalization patterns of Burmese scapolites. The upper crust values from Rudnick and Gao (2003) [23].

5. Discussion

5.1. Chemical Composition of Scapolite

The Burmese scapolites are plotted by the content of the end element components (Figure 9), from which it is known that Burmese scapolites are close to the end of marialite and are a kind of Cl-rich dipyre.

The scapolite exhibits the largest meiotic variation in the meionite–marialite solid solution. The composition of scapolite ($X_4[Y_{12}O_{24}]Z$) is usually described by the molar fraction of Cl at the Z site and the equivalent calcium feldspar content. The former is denoted by XCl= 100 × Cl/ (Cl + S + C) and the latter by EqAn = 100 × (Al − 3)/3. Figure 10a shows the variation of XCl% and EqAn% of equivalent calcium feldspar in scapolite. Ca is strongly positively correlated with EqAn, R^2 = 0.4089 (Figure 10b). Na is lightly positively correlated with EqAn, R^2 = 0.201 (Figure 10c), and K is not significantly negatively correlation with EqAn, R^2 = 0.0242 (Figure 10d). These provide a basis for the complex coupling substitutions observed in the scapolite. The scapolite grains analyzed in this study show consistency. The Cl content varies continuously from 2.55 wt% to 2.73 wt% (0.65–0.71 apfu), indicating that Burmese scapolites (U-1 and U-2) are classified as the chloride-rich scapolite series. The SO_3 content ranges from 0.92 wt% to 1.26 wt% (0.11 to 0.15 apfu), and the C* content (calculated by C* = 1 – Cl − S [24]) ranges from 0.14 apfu to 0.22 apfu.

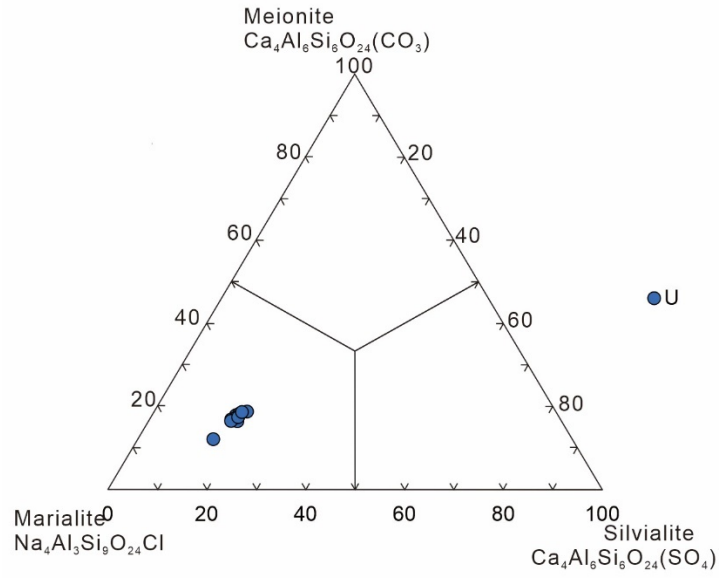

Figure 9. Three end elements illustration of scapolite (Meionite−Marialite−Silvialite). (Burmese scapolites are mainly concentrated in the left end member in the figure and belong to dipyre).

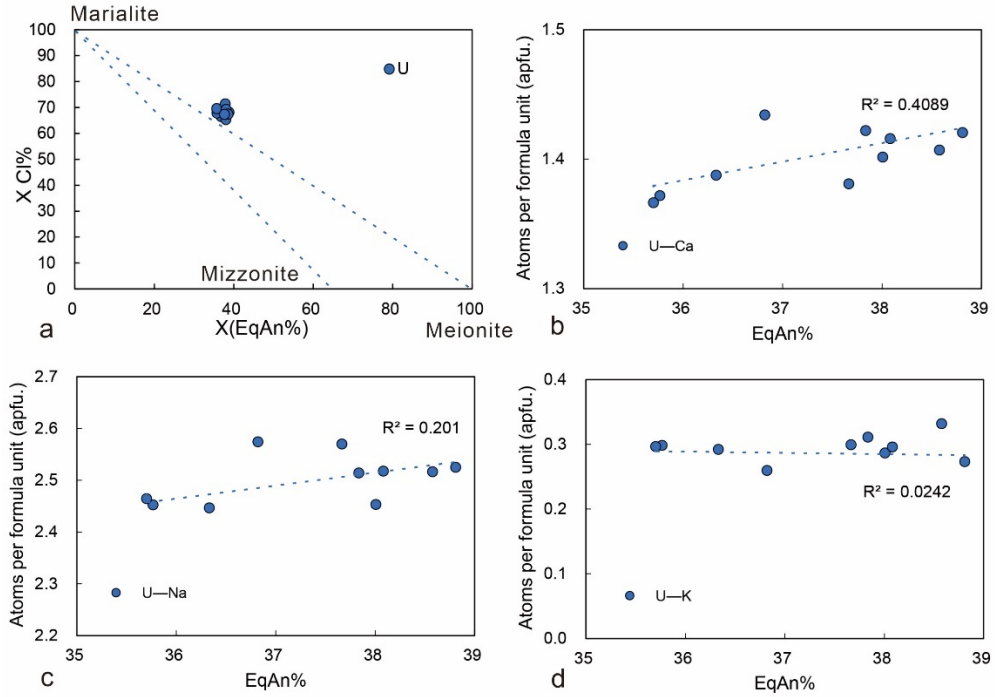

Figure 10. (**a**) The variation of XCl% and EqAn% of equivalent calcium feldspar in scapolite. (**b**–**d**) Relationships between Ca, Na, K and EqAn% in scapolite.

According to Table 2, the light and heavy rare earth element ratio (ΣLREE/ΣHREE) of Burmese scapolites range from 21.56 to 28.33. Moreover, the normalized distribution pattern of REEs in the average upper continental crust shows an obvious right slope trend, which indicates a high degree of LREE and HREE differentiation in Burmese scapolites. In addition, the Burmese scapolites have distinct positive Eu anomalies, which may be due to the ion exchange between fluids in the scapolite and plagioclase [25,26]. As the ore-forming system gradually turns from closed to oxidized, the δEu values increase, forming positive Eu anomalies. The primitive mantle normalization pattern of the Burmese scapolites shows a significant depletion of high field strength element Ta, reflecting that the magma may be contaminated by crustal materials or fluid metasomatism related to subduction [27,28].

Furthermore, overall, the trace elements of Burmese scapolites are closer to and more K-rich than the average upper continental crust values, compared to the primary mantle values.

5.2. Comparison of Scapolite from Different Origins

In this study, the samples from the Zhongtiao Mountains [4] in the southern part of the North China orogenic belt and scapolite from Skallen, East Antarctica [5] were compared with the samples from Myanmar. According to Table 3, the Me% of Zhongtiao Mountains scapolites is 29.99–34.17%, belonging to dipyre; while the Me% of scapolites from East Antarctica is 56.70–61.60%, belonging to mizzonite. The variation of XCl% and EqAn% in Burmese, Zhongtiao Mountains, and East Antarctic scapolites are shown in Figure 11a. It is obvious that the Burmese scapolites and Zhongtiao Mountains scapolites belong to the same type of dipyre with similar Me% content, while the scapolites in East Antarctica with higher Me% content belong to mizzonite. The relationship between Al, Na, Ca, and K contents and the Cl content of different origins can be seen in Figure 11b. In generally, there is a weak negative relation between Al and Cl, a positive relation between Na and Cl contents, a negative relation between Ca and Cl, and no significant relationship between K and Cl.

Table 3. Electron microprobe analysis of scapolite from other origins. Data derived from [4,5].

	BZ50-1	**BZ50-2**	**BZ50-3**	**BZ50-4**	**BZ50-5**	**scp1**	**scp2**	**scp3**	**scp4**	**scp5**
SiO_2	54.07	54.34	54.56	53.84	53.64	50.83	50.12	50.20	50.73	50.64
Al_2O_3	23.06	22.76	22.42	22.88	22.86	25.76	26.01	25.92	26.20	26.47
FeO	0.04	0.17	0.11	0.14	0.01	0.01	0.07	0.04	0.02	bdl
CaO	9.14	8.89	8.50	7.86	9.10	12.79	13.34	13.85	13.70	14.15
Na_2O	9.21	9.31	9.69	9.52	9.24	5.38	4.87	4.92	4.81	4.85
K_2O	0.79	0.85	0.82	0.94	0.83	1.90	1.78	1.71	1.64	1.72
Cl	2.48	2.61	2.67	2.85	2.40	1.90	1.85	1.75	1.82	1.85
SO_3	0.43	0.40	0.30	0.35	0.49	bdl	bdl	bdl	bdl	bdl
O=Cl	0.57	0.60	0.61	0.65	0.55	0.94	0.83	0.79	0.82	0.83
CO_2	1.72	1.57	1.55	1.25	1.75	bdl	bdl	bdl	bdl	bdl
Total	100.37	100.30	100.01	98.98	99.78	97.64	97.78	97.61	98.09	98.84
Cations calculated on the Basis of 16 cations (apfu)										
Si^{4+}	7.87	7.92	7.94	7.91	7.85	7.54	7.44	7.48	7.53	7.46
Al^{3+}	3.96	3.91	3.85	3.96	3.94	4.51	4.55	4.55	4.59	4.60
Ca^{2+}	1.43	1.39	1.33	1.24	1.43	2.03	2.12	2.21	2.18	2.23
Na^{+}	2.60	2.63	2.73	2.71	2.62	1.55	1.40	1.42	1.39	1.39
K^{+}	0.15	0.16	0.15	0.18	0.16	0.36	0.34	0.33	0.33	0.31
Cl^{-}	0.61	0.64	0.66	0.71	0.60	0.48	0.47	0.44	0.46	0.46
SO_3	0.05	0.04	0.03	0.04	0.05	0.00	0.00	0.00	0.00	0.00
CO_2	0.34	0.31	0.31	0.25	0.35	0.00	0.00	0.00	0.00	0.00
Me	34.17	33.23	31.47	29.99	33.94	56.70	60.23	60.88	61.06	61.60
EqAn	31.89	30.27	28.21	32.09	31.47	49.60	51.80	51.30	51.40	52.50

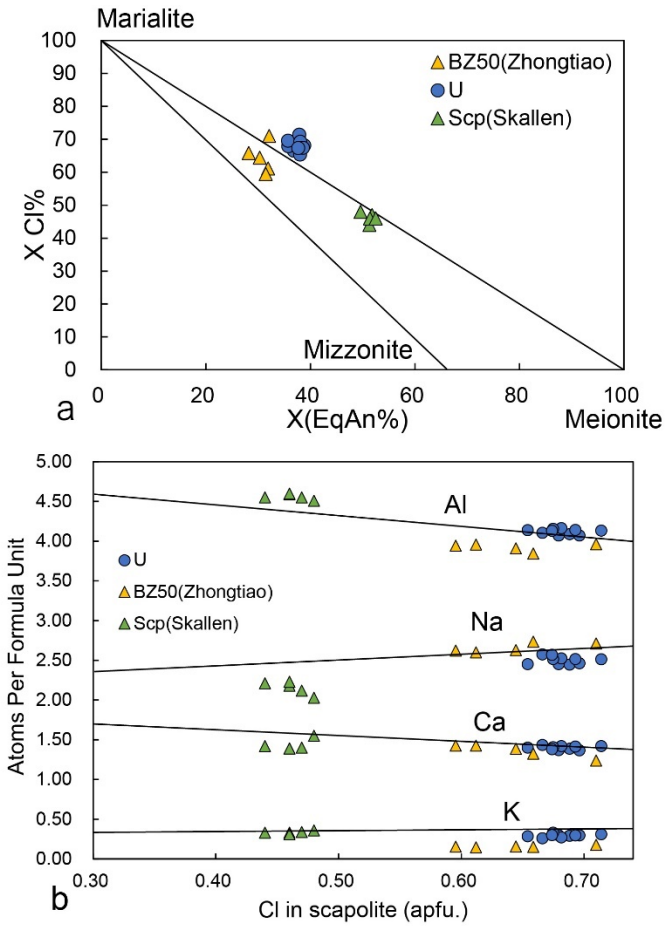

Figure 11. (**a**) The variation of XCl% and EqAn% of equivalent calcium feldspar in scapolite (Mogok, Zhongtiao Mountains and Skallen, East Antarctica). (**b**) Variation of Al, Na, Ca, and K contents in relation to Cl content in the three origins of scapolites.

The overall trend of Al and Cl with Na + K for the samples of this study and the other sources of scapolite is shown in Figure 12. Al was negatively correlated with Na + K, while Cl was positively correlated with Na + K, which indicated that the composition of scapolites is controlled by a general exchange mechanism, such as plagioclase [29]. According to the exchange reaction ($Na_{2.4}Si_{1.4}Cl \rightleftharpoons Ca_{2.4}Al_{1.4}CO_3$) proposed by Rebbert [30], there may be slight but significant differences in the solid solution of scapolites from different occurrences. It can be demonstrated that the coupling degree of each exchange reaction ($NaCa_{-1}$, $SiAl_{-1}$ and $Cl\ (CO_3)_{-1}$) depends on the metamorphic environment (such as temperature and pressure) during the growth of scapolite. In the formation of Cl-containing hornblende and biotite, the complex coupling of the exchange mechanism has a similar dependence on temperature and pressure [31,32]. There is an obvious relationship between temperature, pressure, and the coupling degree between the exchange components of Cl-containing scapolite, hornblende, and biotite, which can be used for geothermal temperature measurement of chloric minerals. However, more data are required to estimate and qualify the temperature and pressure dependence of the exchange mechanism of scapolite.

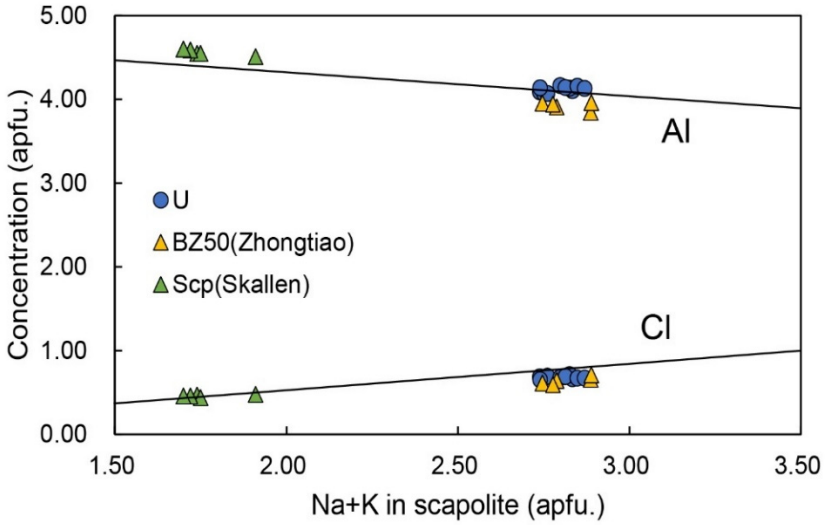

Figure 12. Variation of Al, Cl, and Na + K of scapolites from different origins (Al is negatively correlated with Na + K and Cl is positively correlated with Na + K for the three origins of scapolites).

The trace elements of the Zhongtiao Mountains and Skallen scapolites can be seen in Table 4. Based on REE distribution pattern of scapolites from different origins (Figure 13), it was found that the scapolites from Myanmar and Skallen both showed a right-sloping distribution trend, and the enrichments of LREEs in both were similar, but the HREEs in Skallen scapolites were more deficient. This suggests that the larger ΣLREE/ΣHREE ratios of Skallen scapolites have greater differentiation degrees of LREE and HREE in the region. In contrast, for the scapolites from the Zhongtiao Mountains, the curves showed a left-sloping trend with a relative enrichment in HREEs [33]. The difference between Zhongtiao Mountains and the other two origins may be that the BZ50 (Zhongtiao) was formed in a rock buffer system, while the U (Myanmar) and Scp (Skallen) were formed in a fluid buffer system [4]. The U (Myanmar) δEu = 2.11–3.42, the Scp (Skallen) δEu range is 2.38–5.57, and the BZ50 (Zhongtiao Mountain) δEu = 1.58–1.84. There are obvious positive Eu anomalies in scapolites from three origins, with the Skallen area showing the strongest positive Eu anomalies, which indicates that the degree of oxidation in the metallogenic environment of scapolites is Skallen > Myanmar > Zhongtiao Mountains.

Table 4. Chemical composition of scapolite from other origins by LA-ICP-MS. Data derived from [4,5].

	BZ50-1	**BZ50-2**	**BZ50-3**	**BZ50-4**	**BZ50-5**		**scp1**	**scp2**	**scp3**	**scp4**	**scp5**
Li	0.74	0.59	0.63	0.74	0.67	Li	14	13	13	13	13
Na	62,305.42	63,005.39	63,634.63	64,844.90	65,225.70	Be	5.3	5.9	9.5	7.4	6.9
Mg	25.38	65.01	57.74	494.42	29.11	B	16	22	17	20	18
Al	130,495.14	129,612.49	130,012.13	127,570.26	128,223.58	P	23	19	15	18	13
Cl	26,234.26	27,058.42	27,508.21	29,131.20	29,514.03	Sc	1.3	1.2	1.3	1.2	1.3
K	6342.13	6562.47	6663.76	7356.78	7068.17	Ti	31	63	65	57	59
Ca	65,756.04	63,840.33	63,184.27	59,938.28	59,160.19	V	0.03	0.09	0.05	0.04	0.07
Mn	124.75	122.14	122.84	128.15	122.35	Rb	17	9.29	11	8	8.7
Fe	364.30	447.88	415.35	962.98	397.30	Sr	393	435	342	407	356
Zn	1.26	24.07	1.22	1.74	0.88	Y	1.2	0.35	0.47	1.1	0.54
Ga	8.05	8.17	8.30	8.08	8.05	Zr	0.02	0.05	<0.02	<0.02	0.02
Br	49.19	52.87	63.74	56.56	48.49	Nb	0.003	0.004	<0.01	<0.01	<0.01

Table 4. *Cont.*

	BZ50-1	BZ50-2	BZ50-3	BZ50-4	BZ50-5		scp1	scp2	scp3	scp4	scp5
Rb	1.26	1.84	1.43	3.81	1.36	Cs	0.07	0.05	0.04	0.04	<0.01
Sr	104.10	105.30	103.61	107.31	109.92	Ba	215	142	133	116	95
Y	10.39	10.17	9.74	10.61	8.04	La	21	18	11	16	11
Zr	0.00	24.16	26.48	83.44	7.22	Ce	36	24	17	28	20
Ba	30.55	32.76	32.71	40.37	37.83	Pr	3.5	1.9	1.5	2.5	1.8
La	1.38	1.39	1.54	1.85	1.81	Nd	12	5.4	4.9	8	6.2
Ce	3.81	3.91	4.20	5.19	5.15	Sm	1.8	0.56	0.56	0.98	0.82
Pr	0.60	0.62	0.67	0.83	0.82	Eu	0.7	0.5	0.42	0.53	0.5
Nd	3.05	3.02	3.27	3.80	3.96	Gd	0.9	0.27	0.32	0.53	0.41
Sm	1.20	1.22	1.30	1.50	1.35	Tb	0.07	0.02	0.02	0.05	0.03
Eu	0.67	0.64	0.68	0.68	0.69	Dy	0.27	0.07	0.1	0.22	0.13
Gd	2.15	2.10	2.12	2.32	1.95	Ho	0.04	0.01	0.02	0.03	0.02
Tb	0.43	0.42	0.42	0.47	0.39	Er	0.08	0.03	0.04	0.08	0.04
Dy	2.44	2.37	2.24	2.53	2.01	Tm	0.01	0.004	0.00	0.00	0.00
Ho	0.46	0.46	0.45	0.49	0.39	Yb	0.04	0.02	0.00	0.00	0.00
Er	0.98	0.99	0.96	1.14	0.76	Lu	0.01	0.00	0.00	0.00	0.00
Tm	0.11	0.13	0.13	0.16	0.10	Hf	<0.01	<0.01	<0.04	<0.04	<0.04
Yb	0.53	0.73	0.69	1.03	0.48	Ta	<0.01	<0.01	<0.02	<0.02	<0.02
Lu	0.07	0.11	0.10	0.20	0.06	Pb	40	53	36	38	34
Hf	b.d	0.72	0.81	2.48	0.21	Th	0.03	0.13	0.02	0.04	<0.02
Pb	4.53	1.02	1.37	1.06	0.58	U	0.01	0.01	<0.02	<0.02	<0.02
δEu	1.82	1.73	1.77	1.58	1.84	δEu	2.38	5.58	4.30	3.19	3.74

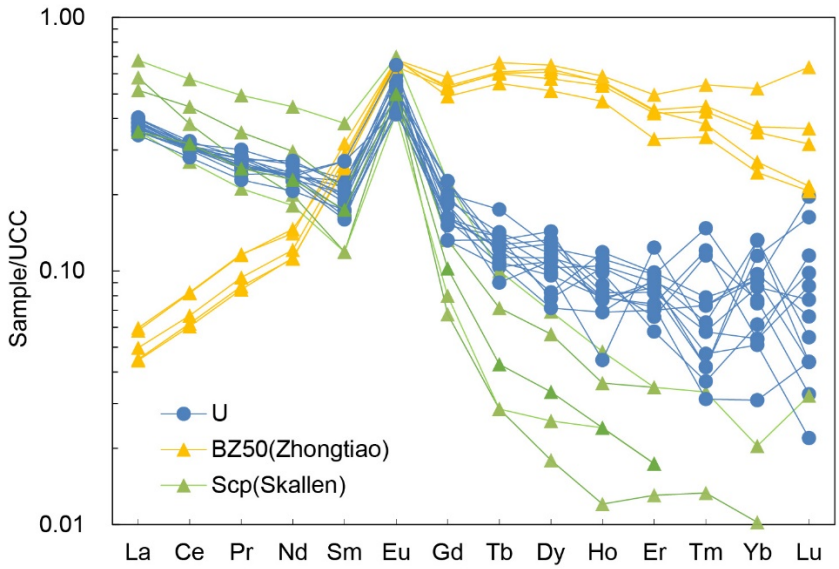

Figure 13. Average upper continental crust-normalized REE distribution patterns of scapolites (Mogok, Zhongtiao Mountains and Skallen, East Antarctica). The normalization values for upper continental crust are from Rudnickand and Gao (2003) [23].

5.3. Volatile Fraction in Scapolite

Volatile components play an important role in rock-formation and mineralization. They not only act as carriers in the deep crust but also have frequent redox interactions with other components. Thus, volatile components can change the material composition of the lower crust [33–36].

It is generally accepted that the formation of scapolite is accompanied by low activity of αH_2O and significant activity of αCl^- and $\alpha(CO_3)^{2-}$, with the possible presence of SO_3. The formation of scapolite is often accompanied by the presence of volatile-rich fluids [37,38]. Kullerud and Eramert [29] indicated that chlorite-bearing minerals are the result of rapid crystallization under isobaric and isothermal conditions. Compared with amphibole and biotite in basal rocks, Cl is more likely to present in the fluids. In a closed system, the Cl content of pre-crystallized minerals is low, which makes the Cl content and $\alpha Cl^-/\alpha OH^-$ value in the fluid gradually increase. Then Cl begins to enter amphibole and biotite: $X(OH^-) + HCl = X(Cl^-) + H_2O$, where X represents amphibole or biotite [39]. As the value of $\alpha Cl^-/\alpha OH^-$ is further increased, the scapolite crystallizes and absorbs most of the remaining Cl, when the components are suitable. With the crystallization of amphibole and biotite, the CO_2 content in the fluids gradually increases, and the most of them will be consolidated in the scapolite [29]. Furthermore, the relationship between the scapolite composition and the contents of Cl^- and CO_3^{2-} (according to the coupling effect of substitution) [32] is as follows: Na ⇋ Ca, Si ⇋ Al and Cl ⇋ CO_3^{2-}, namely $NaCl_{\ scapolite} + CaCO_{3\ fluid} \leftrightharpoons CaCO_{3\ scapolite} + NaCl_{\ fluid}$, which makes the entry of CO_3^{2-} to dilute the Cl in scapolite. Therefore, the component of scapolite is mainly governed by the ratio of $\alpha Cl^-/\alpha(CO_3)^{2-}$ in the fluids. If the substitutions of Na ⇋ Ca and Si ⇋ Al in scapolite reach a balance with plagioclase, the activity of Cl as a small component will control the content of scapolite [40–43].

6. Conclusions

The Burmese scapolites are colorless (with a yellow tone), with good crystal morphology, and they have high scientific value. Although the hardness of scapolite is low, it is still highly attractive to collectors. The study of the gemological properties of the scapolite can be enriched by spectroscopic tests, which can supplement information on the origin of Mogok scapolites from Myanmar. The measurement of major and trace elements can provide insight into the characteristics of Burmese scapolites in terms of species, volatile fraction, and REEs.

According to the spectral test results, the infrared spectrum of the samples is mainly Si-O and Al-O vibration at 400–1300 cm^{-1}; the vibration spectrum of CO_3^{2-} ion is shown at 1400–3000 cm^{-1}; at 3000–3700 cm^{-1} it is the stretching vibration of M-OH and O-H. There are 13 group of absorption peaks in the Raman spectrum, and the peaks below 400 cm^{-1} are split due to the influence of Al^{VI}; the peaks from 400 cm^{-1} to 800 cm^{-1} are caused by Si (Al)-O-Si (Al) vibrations; while the peaks near 992 cm^{-1} and 1110 cm^{-1} are caused by sulfate ion and carbonate ion vibrations, respectively. Furthermore, the Burmese scapolites have more ordered Al than the Pakistani scapolites. The yellow tone of Burmese scapolites may be caused by the electronic transition of metal ion Fe^{3+}, or it may be contaminated by Fe-containing substances. Moreover, the dark inclusions in the samples can be identified as graphite.

Based on the results of major elements, it is clear that the Burmese scapolite is a dipyre rich in Cl. The composition of scapolite is mainly influenced by $\alpha Cl^-/\alpha\ (CO_3)^{2-}$ in fluid. Furthermore, the activity degree of Cl will control the scapolite content if the exchange between scapolite and plagioclase reaches a balance. According to the trace elements test results, the REEs of the Burmese scapolite show enrichment of LREE and depletion in HREE with an obvious positive Eu anomaly. This demonstrates that ion exchange may have occurred between fluids in the scapolite and plagioclase, and the metallogenic environment of scapolite in Myanmar is oxidized.

Author Contributions: Writing—original draft, P.Y.; writing—review and editing, P.Y., Y.Z. and B.X.; data curation, P.Y., Y.Z. and J.S.; software, P.Y.; methodology, P.Y. and Y.Z.; resources, B.X. All authors have read and agreed to the published version of the manuscript.

Funding: This research was funded by National Key Technologies R&D Program (2020YFA0714800, 2019YFA0708602); National Natural Science Foundation of China (42073038, 41803045), Young Talent Support Project of CAST, the Fundamental Research Funds for the Central Universities (Grant no. 265QZ2021012), and IGCP-662.

Data Availability Statement: The data presented in this study are available within the article.

Acknowledgments: We thank the editor and reviewers for constructive comments which helped in improving our paper. This is the 10th contribution of B.X. for the National Mineral Rock and Fossil Specimens Resource Center.

Conflicts of Interest: The authors declare no conflict of interest.

References

1. Superchi, M.; Pezzotta, F.; Gambini, E.; Castaman, E. Yellow Scapolite from Ihosy, Madagascar. *Gems Gemol.* **2010**, *46*, 274–279. [CrossRef]
2. Teertstra, D.K.; Schindler, M.; Sherriff, B.L.; Hawthorne, F.C. Silvialite, a New Sulfate-Dominant Member of the Scapolite Group with an Al-Si Composition near the 14/ m–P42/n Phase Transition. *Mineral. Mag.* **1999**, *63*, 321–329. [CrossRef]
3. Ren, L.D.; Gao, Y. Formation of scapolite in plagioclase amphibolite in southwest Kunlun Interaction with fluid volatiles. *Acta Petorlogica Mineral.* **2002**, *21*, 398–406.
4. Qiu, Z.; Fan, H.-R.; Tomkins, A.; Brugger, J.; Etschmann, B.; Liu, X.; Xing, Y.; Hu, Y. Insights into Salty Metamorphic Fluid Evolution from Scapolite in the Trans-North China Orogen: Implication for Ore Genesis. *Geochim. Cosmochim. Acta* **2021**, *293*, 256–276. [CrossRef]
5. Satish-Kumar, M.; Hermann, J.; Tsunogae, T.; Osanai, Y. Carbonation of Cl-Rich Scapolite Boudins in Skallen, East Antarctica: Evidence for Changing Fluid Condition in the Continental Crust. *J. Metamorph. Geol.* **2006**, *24*, 241–261. [CrossRef]
6. Searle, M.P.; Garber, J.M.; Hacker, B.R.; Htun, K.; Gardiner, N.J.; Waters, D.J.; Robb, L.J. Timing of Syenite-Charnockite Magmatism and Ruby and Sapphire Metamorphism in the Mogok Valley Region, Myanmar. *Tectonics* **2020**, *39*, e2019TC005998. [CrossRef]
7. Keller, P.C. The Rubies of Burma: A Review of the Mogok Stone Tract. *Gems Gemol.* **1983**, *19*, 209–219. [CrossRef]
8. Waltham, T. The Ruby Mines of Mogok. *Geol. Today* **1999**, *15*, 143–149. [CrossRef]
9. Oo, T.Z. Geology and Gems of Mogok Area, Pyin Oo Lwin District, Mandalay Region. Ph.D. Thesis, Monywa University, Monywa, Myanmar, 2015.
10. Thu, Y.K.; Enami, M. Evolution of Metamorphic Fluid Recorded in Granulite Facies Metacarbonate Rocks from the Middle Segment of the Mogok Metamorphic Belt in Central Myanmar. *J. Metamorph. Geol.* **2018**, *36*, 905–931. [CrossRef]
11. Thu, Y.K.; Enami, M.; Kato, T.; Tsuboi, M. Granulite Facies Paragneisses from the Middle Segment of the Mogok Metamorphic Belt, Central Myanmar. *J. Mineral. Petrol. Sci.* **2017**, *112*, 1–19. [CrossRef]
12. Deng, X.Y. Gemmological Characteristics and Luminescence of Scapolite. Master's Thesis, China University of Geosciences, Beijing, China, 2019.
13. Xie, J. Fine structure of Aluminosilicate and Raman Spectroscopy of Feldspar. Master's Thesis, China University of Geosciences, Beijing, China, 2008.
14. Culka, A.; Jehlička, J. A Database of Raman Spectra of Precious Gemstones and Minerals Used as Cut Gems Obtained Using Portable Sequentially Shifted Excitation Raman Spectrometer. *J. Raman Spectrosc.* **2019**, *50*, 262–280. [CrossRef]
15. Hofmeister, A.M.; Rossman, G.R. Color of feldspars. *Rev. Mineral.* **1980**, *2*, 271–280.
16. Burns, R.G. *Mineralogical Applications of Crystal Field Theory; Cambridge Topics in Mineral Physics and Chemistry*, 2nd ed.; Cambridge University Press: Cambridge, UK; New York, NY, USA, 1993; ISBN 9780521430777.
17. Cao, Y. Study on Feldspar and Its Color Improvement in Guyang County, Inner Mongolia Autonomous Region. Master's Thesis, China University of Geosciences, Beijing, China, 2006.
18. Krzemnicki, M. Red and Green Labradorite Feldspar from Congo. *J. Gemmol.* **2004**, *29*, 15–23. [CrossRef]
19. Ren, Q.Q.; Chen, M.H.; Li, X.Y. Analysis of chemical composition and heat treatment results of light yellow scapolite. *J. Gemstones Gemol.* **2016**, *18*, 34–39.
20. Gu, X.Z.; Qiu, Z.L.; Li, Y.D.; Yang, P.; Li, L.F. Graphite inclusions in jade excavated from the tomb of King Chu at Lion Mountain, Western Han Dynasty. *J. Zhongshan Univ. Nat. Sci. Ed.* **2007**, *6*, 141–142.
21. Sokolova, E.; Hawthorne, F.C. The crystal chemistry of the scapolite-group minerals. I. Crystal structure and long-range order. *Can. Mineral.* **2008**, *46*, 1527–1554. [CrossRef]
22. Seo, J.H.; Guillong, M.; Aerts, M.; Zajacz, Z.; Heinrich, C.A. Microanalysis of S, Cl, and Br in Fluid Inclusions by LA–ICP-MS. *Chem. Geol.* **2011**, *284*, 35–44. [CrossRef]
23. Rudnick, R.L.; Gao, S.; Holland, H.D.; Turekian, K.K. Composition of the continental crust. *Crust.* **2003**, *3*, 1–64.

24. Bryden, C.D.; Jamieson, R.A. Scapolite Pegmatite from the Nordøyane Ultra-High Pressure Domain, Western Gneiss Region, Norway: Partial Melting Driven by Infiltration of Mantle-Derived Fluid. *Lithos* **2020**, *364–365*, 105546. [CrossRef]
25. Yuan, P.; Xu, B.; Wang, Z.; Liu, D. A Study on Apatite from Mesozoic Alkaline Intrusive Complexes, Central High Atlas, Morocco. *Crystals* **2022**, *12*, 461. [CrossRef]
26. Xu, B.; Hou, Z.Q.; Griffin, W.L.; Lu, Y.; Belousova, E.; Xu, J.F.; O'Reilly, S.Y. Recycled volatiles determine fertility of porphyry deposits in collisional settings. *Am. Mineral.* **2020**, *106*, 656–661. [CrossRef]
27. Qiu, C.Y.; Xiao, Q.R.; Wei, Y.F.; Luo, W.; Yang, Y.M.; Xiao, Y.F. LA-ICP-MS zircon U-Pb dating, geochemistry and geological significance of the Late Cretaceous eclogite in the Bejorzecuo area, northwest margin of the Gondwana Belt. *J. Geol.* **2018**, *92*, 2215–2226.
28. Xu, B.; Griffin, W.L.; Xiong, Q.; Hou, Z.-Q.; O'Reilly, S.Y.; Guo, Z.; Pearson, N.J.; Gréau, Y.; Yang, Z.-M.; Zheng, Y.-C. Ultrapotassic Rocks and Xenoliths from South Tibet: Contrasting Styles of Interaction between Lithospheric Mantle and Asthenosphere during Continental Collision. *Geology* **2017**, *45*, 51–54. [CrossRef]
29. Kullerud, K.; Erambert, M. Cl-Scapolite, Cl-Amphibole, and Plagioclase Equilibria in Ductile Shear Zones at Nusfjord, Lofoten, Norway: Implications for Fluid Compositional Evolution during Fluid-Mineral Interaction in the Deep Crust. *Geochim. Cosmochim. Acta* **1999**, *63*, 3829–3844. [CrossRef]
30. Rebbert, C.R.; Rice, J.M. Scapolite-Plagioclase Exchange: Cl-CO_3 Scapolite Solution Chemistry and Implications for Peristerite Plagioclase. *Geochim. Cosmochim. Acta* **1997**, *61*, 555–567. [CrossRef]
31. Kullerud, K. Occurrence and origin of Cl-rich amphibole and biotite in the Earth's crust—Implications for fluid composition and evolution. *Hydrogeol. Cryst. Rocks* **2000**, *34*, 205–225.
32. Chupin, V.P.; Kuz'min, D.V.; Madyukov, I.A. Melt Inclusions in Minerals of Scapolite-Bearing Granulite (Lower Crustal Xenoliths from Diatremes of the Pamirs). *Dokl. Earth Sci.* **2006**, *407*, 507–511. [CrossRef]
33. Xu, B.; Hou, Z.Q.; Griffin, W.L.; O'Reilly, S.Y. Apatite halogens and Sr–O and zircon Hf–O isotopes: Recycled volatiles in Jurassic porphyry ore systems in southern Tibet. *Chem. Geol.* **2022**, *605*, 120924. [CrossRef]
34. Xu, B.; Kou, G.; Etschmann, B.; Liu, D.; Brugger, J. Spectroscopic, Raman, EMPA, Micro-XRF and Micro-XANES Analyses of Sulphur Concentration and Oxidation State of Natural Apatite Crystals. *Crystals* **2020**, *10*, 1032. [CrossRef]
35. Touret, J.L.R. Mantle to Lower-Crust Fluid/Melt Transfer through Granulite Metamorphism. *Russ. Geol. Geophys.* **2009**, *50*, 1052–1062. [CrossRef]
36. Newton, R.C. Young and Old Granulites: A Volatile Connection. *J. Geol.* **2020**, *128*, 395–413. [CrossRef]
37. Xu, B.; Hou, Z.-Q.; Griffin, W.L.; Zheng, Y.-C.; Wang, T.; Guo, Z.; Hou, J.; Santosh, M.; O'Reilly, S.Y. Cenozoic Lithospheric Architecture and Metallogenesis in Southeastern Tibet. *Earth-Sci. Rev.* **2021**, *214*, 103472. [CrossRef]
38. Kassoli-Fournaraki, A. Ca-Rich Scapolite in Quartz Amphibolites from the Sarti Area, Northern Greece. *Eur. J. Mineral.* **1991**, *3*, 887–894. [CrossRef]
39. Zhu, C.; Sverjensky, D.A. Partitioning of F-Cl-OH between Minerals and Hydrothermal Fluids. *Geochim. Cosmochim. Acta* **1991**, *55*, 1837–1858. [CrossRef]
40. Vanko, D.A.; Bishop, F.C. Occurrence and Origin of Marialitic Scapolite in the Humboldt Lopolith, N.W. Nevada. *Contrib. Mineral. Petrol.* **1982**, *81*, 277–289. [CrossRef]
41. Jiang, S.-Y.; Palmer, M.R.; Xue, C.-J.; Li, Y.-H. Halogen-Rich Scapolite-Biotite Rocks from the Tongmugou Pb-Zn Deposit, Qinling, Northwestern China: Implications for the Ore-Forming Processes. *Mineral. Mag.* **1994**, *58*, 543–552. [CrossRef]
42. Xu, B.; Hou, Z.-Q.; Griffin, W.L.; O'Reilly, S.Y.; Zheng, Y.-C.; Wang, T.; Bin-Fu; Xu, J.-F. In-Situ Mineralogical Interpretation of the Mantle Geophysical Signature of the Gangdese Cu-Porphyry Mineral System. *Gondwana Res.* **2022**, *111*, 53–63. [CrossRef]
43. Fleet, M.E.; Liu, X.; Harmer, S.L.; King, P.L. Sulfur k-edge xanes spectroscopy: Chemical state and content of sulfur in silicate glasses. *Can. Mineral.* **2005**, *43*, 1605–1618. [CrossRef]